Influence of 1 wt-% addition of Ni on structural and mechanical properties of ferritic ductile irons

J. Lacaze*[1], P. Larrañaga[2], I. Asenjo[2], R. Suárez[2] and J. Sertucha[2]

Two sets of ductile irons with and without Ni additions containing various low Si contents have been prepared in order to study the effect of Ni on structural and mechanical properties of thermal analysis cups and standard keel blocks. Because contradictory results appearing in literature, this work has been focused on the influence of this element on matrix structure and on impact properties at room temperature as well as at low temperatures. The structures of Ni free and Ni bearing alloys have been related to the features of cooling curves recorded on both casting types and to the tensile and impact properties of the materials.

Keywords: Nodular cast iron, Ferritic matrix, Pearlite, Mechanical properties, Low temperature, Impact properties

Introduction

In recent years some foundries have reported attempts to use nickel for improving impact properties, without verifiable results though. Such attempts seem sustained by the fact that nickel has been known since long to improve low temperature impact properties of pure iron.[1] In contrast, the ASM handbook[2] and Angus[3] both report that nickel increases the transition temperature, and thus negatively affects impact properties. Neither of these reports gives any details on the nature of the matrix, namely, the amount of ferrite and pearlite. As a matter of fact, the only result found up to now for a fully ferritised matrix shows Ni to slightly decrease room temperature (RT) impact energy,[4] without any information on its effect on the brittle to ductile transition temperature.

Consideration of matrix structure is important since pearlite is expected to have a detrimental effect on impact properties while improving yield stress Y and ultimate tensile stress (UTS). In the ASM handbook on cast iron[5] three graphs show that nickel addition up to 2 wt-% improves Y, UTS and hardness of ductile irons at RT. It is further seen that this improvement applies to as cast, normalised and annealed materials, which makes Ni a very potent alloying element. The original data are however not available and other works on the effect of Ni show some incoherencies. Small additions of Ni were claimed to promote the formation of ferrite and increase ductility,[6] while other studies show the opposite[4,7–9] conclusions that Ni increases Y and UTS. In a previous work on the effect of various additions on pearlitic nodular cast iron,[10] a statistical analysis appeared to show that the addition of Ni up to 1·2 wt-% decreases the UTS without affecting Y and elongation at rupture A. Focusing on a fully ferritic matrix,[11] it was observed that the addition of Ni up to 0·27 wt-% confirmed its positive effect on Y and UTS at RT while it appeared to negatively affect A. In this latter study, no trend could be found as for impact properties, possibly because of the low level of addition. To clarify the role of Ni on mechanical properties at RT and low temperature impact properties, a new series of casting was manufactured with an addition of Ni of 1 wt-% and various Si contents. The effect of Ni on the as cast structure and on properties of as cast and ferritised materials have thus been investigated.

Experimental

In order to facilitate the analysis, alloys with and without Ni addition have been prepared with three levels of silicon (1·4, 1·7 and 1·9 wt-%). For this purpose, 80 kg of base melt was prepared using a medium frequency induction furnace (250 Hz and 100 kW in power) with a charge composed of 36 kg of low alloyed steel scrap, 42 kg of low alloyed pig iron, 1·4 kg of graphite (98·4 wt-%C) and 0·9 kg of $FeSi_{75}$ [75·4Si–0·6Al–0·1C–23·9Fe (wt-%)]. After melting, the batch temperature was increased to 1430°C and a sample was taken for chemical analysis. Carbon and sulphur contents were measured using a Leco-CS200 combustion analyser while all other elements were measured using a Spectrolab spectrometer. The carbon and silicon contents of the melt were adjusted to the required values adding graphite and FeSi directly to the furnace. The final chemical composition of this base melt (MB1) is listed in Table 1.

The batch temperature was increased to 1480°C and a first Mg treatment was performed by pouring ~40 kg of the prepared base metal in a 80 kg capacity ladle in

[1]CIRIMAT, Université de Toulouse, ENSIACET, BP 44362, 31030 Toulouse Cedex 4, France
[2]Área de Ingeniería y Procesos de Fundición, AZTERLAN, Aliendalde Auzunea 6, E-48200 Durango (Bizkaia), Spain

*Corresponding author, email jacques.lacaze@ensiacet.fr

which powder of FeSiMg [grain size (GS) 1–10 mm] was positioned at the bottom and covered with steel scrap foils from stamping processes. The amount of FeSiMg corresponds to 1·1% of the mass of metal poured; its composition is 43·6Si–6·3Mg–1·1Ca–0·6Al–0·9RE (wt-%). After completion of the reaction the batch was skimmed and metal samples were taken for subsequent chemical analysis (medal) and casting of two thermal analysis (TA) cups and two keel blocks were performed. Both TA cups and one of the two keel blocks had a K type thermocouple located close to the geometric centre. Inoculation was performed by adding 0·18 wt-% of a commercial inoculant [GS 0·2–0·6 mm, composition 74·4Si–4·1Al–1·2Ca–0·5RE (wt-%)] in the cups and keel block moulds before pouring. The chemical analysis of the Mg treated melt (T1) is listed in Table 1. Note that the effect of inoculation is not included in this analysis.

After these first castings, the melt in the ladle was transferred back to the melting furnace. Its carbon content was measured and adjusted in order to obtain a similar value to that of the base melt MB1. A second Mg treatment was performed at 1480°C following a similar methodology as described above. The resulting Mg treated batch (T2) was used for casting TA cups and keel blocks in the same way as before. Finally, in a third step, a new alloy was obtained after transferring the remaining melt from the ladle to the furnace. After adjusting the carbon content to a similar value to that of melt MB1 and then increasing the temperature to 1480°C, a third Mg treatment was made on 35 kg of this melt (T3) and the same castings as before were carried out. The chemical compositions of melts T2 and T3 are also listed in Table 1.

Table 1 Chemical analyses of melts, wt-%

Melt	C	Si	Mn	P	S	Cr
MB1	3·98	0·92	0·07	0·012	0·004	0·02
T1	3·83	1·40	0·09	0·012	0·005	0·03
T2	3·77	1·70	0·10	0·013	0·005	0·02
T3	3·75	1·85	0·11	0·014	0·003	0·04
MB2	4·05	0·93	0·10	0·013	0·006	0·03
T4	3·94	1·42	0·12	0·013	0·005	0·04
T5	3·89	1·74	0·11	0·013	0·005	0·03
T6	3·89	1·88	0·13	0·013	0·004	0·05

Melt	Mo	Ni	Cu	Mg	Ti	Sn
MB1	<0·01	0·03	0·01	<0·005	<0·010	<0·005
T1	0·01	0·04	0·01	0·055	<0·010	<0·005
T2	0·01	0·04	0·01	0·056	<0·010	<0·005
T3	0·01	0·05	0·01	0·058	<0·010	<0·005
MB2	<0·01	1·00	0·01	<0·005	<0·010	<0·005
T4	0·01	0·94	0·01	0·054	<0·010	<0·005
T5	0·01	0·93	0·01	0·052	<0·010	<0·005
T6	0·01	0·92	0·02	0·054	<0·010	<0·005

In the second set of experiments, 80 kg of an alloy containing ~1% of Ni was prepared using the same melting furnace and a metallic charge composed by 35 kg of returns, 24 kg of low alloyed steel scrap, 20 kg of low alloyed pig iron, 1·0 kg of graphite (98·4 wt-%C) and 0·8 kg of Ni (99·9 wt-%Ni). After melting the batch temperature was increased to 1450°C and a sample was taken in order to determine the chemical composition and to adjust the carbon and silicon contents to the required values. The chemical composition of the resulting base melt (MB2) is indicated in Table 1. Three alloys containing Ni were prepared and cast according to the methodology described above. Therefore, three successive Mg treated batches (T4, T5 and T6) were obtained at increasing Si content and the corresponding set of cups and keel blocks were poured. Table 1 lists the chemical compositions of these batches.

After cooling, all TA cup samples were cut for subsequent metallographic analysis performed with an optical microscope Leica. Nodule counts N and phase fractions were determined in the central areas where the thermocouples were located using an image analysis software. After counting the nodules, the samples were etched using nital 5 to reveal and characterise the structure of the matrix. Samples for mechanical tests were machined out from as cast keel blocks as indicated in an earlier work[11] for determining UTS, Y, hardness HBW and elongation at rupture A, as well as impact energy at various temperatures between −60°C and RT. Tensile tests were carried out with a ZWICK Z250 apparatus, impact tests with a ZWICK 5111 and hardness was measured with an Instron Wolpert equipment. All impact tests were performed on standard notched samples and were repeated three times. After determining the mechanical properties, all specimens were used for evaluating the graphite nodule count and the structural features in areas close to the fracture surfaces. In all cases, N values, as well as pearlite and ferrite fractions, were estimated as the average of values obtained from five different fields.

The second keel block of each casting test was then ferritised by means of a subcritical anneal and both mechanical tests and metallographic inspections were performed as described above.

Results and discussion

Results from metallographic analysis of as cast TA cups and as cast keel blocks are listed in Table 2. For both types of castings, the matrix consists in pearlite and ferrite located around the graphite nodules as illustrated

Table 2 Metallographic results obtained from TA cups and keel blocks

	TA cups			As cast keel blocks			Heat treated keel blocks			
Melt	N/mm^{-2}	Pearlite/%	Ferrite/%	N/mm^{-2}	Pearlite/%	Ferrite/%	N/mm^{-2}	Pearlite/%	Ferrite/%	GS/μm
T1*	178	66	24	175	17	83	172	<2	>98	45
T2	197	66	34	160	15	85	178	<2	>98	65
T3	256	61	39	162	15	85	191	<2	>98	40
T4*	252	78	20	191	24	76	210	<2	>98	50
T5	360	59	41	147	25	75	195	<2	>98	40
T6	276	56	44	183	17	83	195	<2	>98	50

*Carbides were found in the central areas of the TA cup.

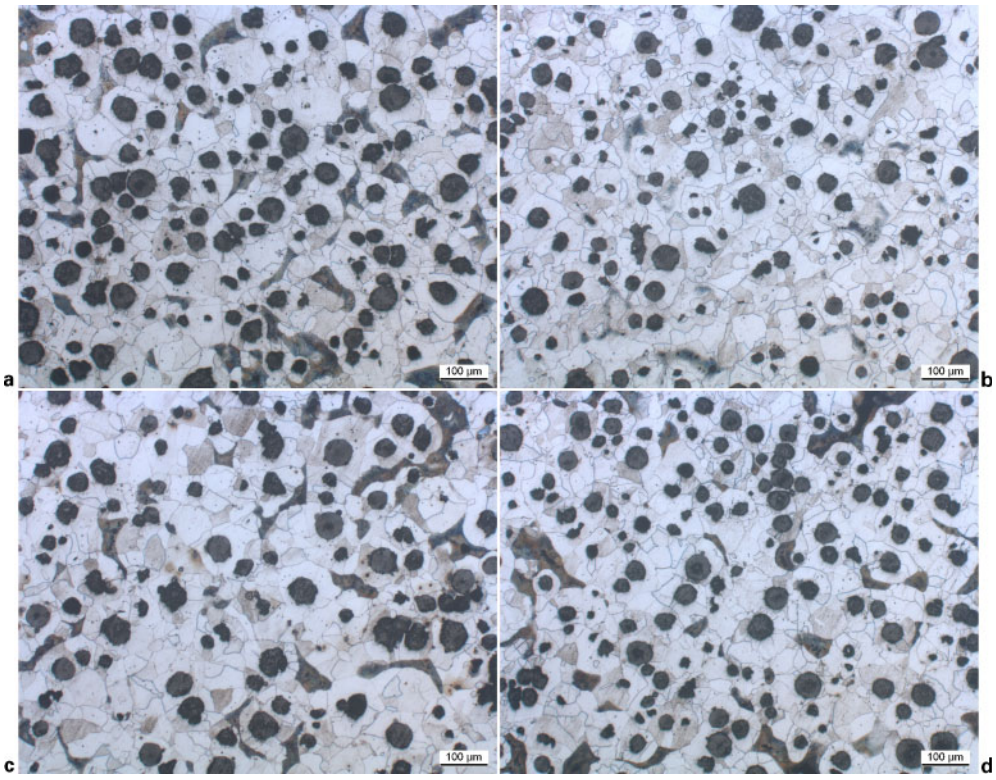

1 Structures of as cast keel blocks with *a* T1, *b* T4, *c* T3 and *d* T6 alloys

in Fig. 1 for keel blocks. It was observed that TA cups cast with T1 and T4 alloys show carbides in the central area (10 and 2% respectively), certainly in relation with their low Si contents. For the TA cups the nodule counts appear higher for melts with Ni, though the value for T5 looks very high. This effect of Ni may be in agreement with its graphitising effect reported in the literature.[12,13] The higher nodule count certainly explains the lower carbide fraction in alloy T4 when compared to alloy T1 and the slightly lower amount of pearlite in the Ni bearing alloys for the two highest silicon contents. As cast keel blocks show similar features although no carbides were found because of the slower cooling rate. The values of N are still larger for the Ni bearing alloys, but the data for T5 which seem by far too low this time. These higher values of N are unexpectedly associated to slightly higher amounts of pearlite in Ni bearing alloys and this pearlite promoter effect is more apparent for the two alloys with lower silicon contents (Table 2).

Figure 2 compares the cooling curves recorded on alloys T1 and T4 cast in keel block. While the addition of Ni was found to slightly increase the temperature of the eutectic arrest, it also clearly shifted the eutectoid transformation to lower temperatures. These features were also observed for the TA cups and the two other couples T2–T5 and T3–T6, although the eutectoid reaction could not be recorded in the case of the T6 TA cup because the thermocouple broke. The eutectic reaction can be characterised by the minimum temperature before recalescence $T_{e,min}$, while the eutectoid reaction may be characterised as described previously[14] by the start temperature $T_{\alpha,exp}$ and either the minimum temperature before recalescence $T_{p,exp}$ or the temperature at which the absolute cooling rate is maximum when there is no recalescence T_{trans}. The indices α and p indicate that it was implicitly considered that the eutectoid transformation starts with ferrite while recalescence is associated with pearlite growth. In the following, T_{trans} will be related to the pearlite reaction when there is no recalescence. This is certainly relevant when the pearlite fraction is high but may not be appropriate at very low cooling rates.[14]

$T_{e,min}$ could be compared to the stable eutectic temperature T_{eut} calculated by means of ThermoCalc software[15] and the TC-Fe_4 database.[16] It is seen in Table 3 that the eutectic undercooling $\Delta T_{eut} = T_{eut} - T_{e,min}$ increases with the cooling rate, from keel blocks to TA cups, while remaining very similar within

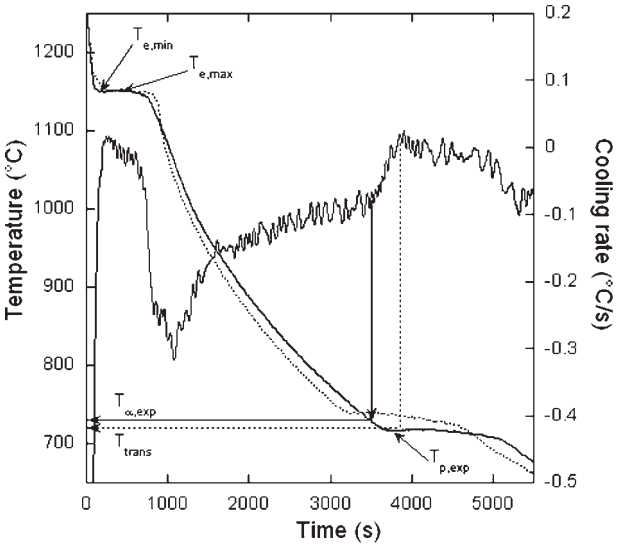

2 Examples of cooling curves recorded on T1 (dotted line) and T4 (solid line) keel blocks, with cooling rate curve for T4: definition of characteristic temperatures is illustrated for T4 curve

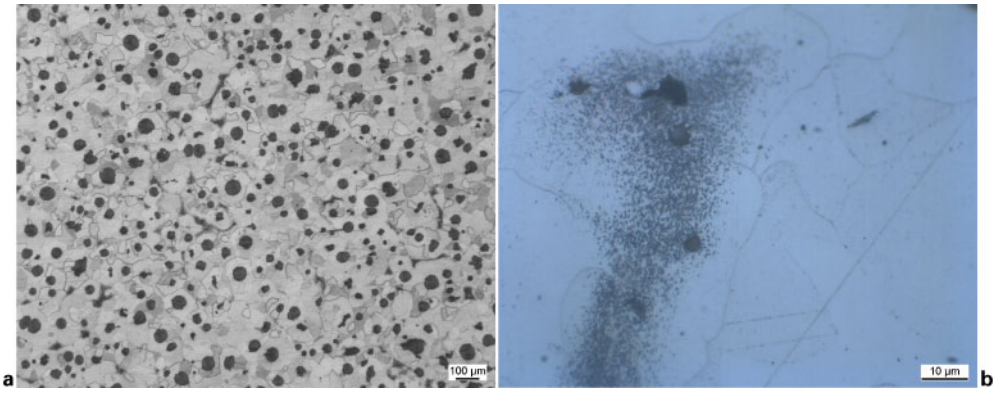

a b

3 Overall microstructure of *a* alloy T6 and detail showing *b* globular-like pearlite

each series of castings, varying from 4·3 to 8·2°C for keel blocks and from 13·5 to 20·2°C for TA cups.

Evaluating $T_{\alpha,exp}$ was not always easy as the start of the eutectoid reaction appeared sometimes very smooth, in particular for records on keel blocks. The data in Table 3 show a clear increase in $T_{\alpha,exp}$ with the Si content when comparing values for T1 and T3 and for T4 and T6, as expected from the well known ferrite promoter effect of Si as this element increases the temperature range of the austenite–ferrite–graphite three-phase field. These data show also a strong decrease in $T_{\alpha,exp}$ with the addition of Ni amounting to 20–30°C. The same effects are also observed when looking at the values reported for $T_{p,exp}$ or T_{trans}, namely, an increase in these values when Si is increased and a decrease by 20–30°C of the corresponding data for a 1 wt-% addition of Ni.

It has been shown previously that the start of the eutectoid reaction should refer to the lowest temperature of the three-phase field, either stable (ferrite–austenite–graphite) for the ferritic reaction or metastable (ferrite–austenite–cementite) for pearlite precipitation.[14,17,18] The respective characteristic temperatures, T_α and T_p (°C), could be evaluated by means of the following equations[19] where the content in i species w_i is expressed in wt-%

$$T_\alpha = 739 + 18.4w_{Si} + 2.0(w_{Si})^2 - 14.0w_{Cu} - 45.0w_{Mn} + 2.0w_{Mo} - 24.0w_{Cr} - 27.5w_{Ni}$$

$$T_p = 727 + 21.6w_{Si} + 0.023(w_{Si})^2 - 21.0w_{Cu} - 25.0w_{Mn} + 8.0w_{Mo} + 13.0w_{Cr} - 33.0w_{Ni}$$

It is seen that these equations agree with the observed effect of both Si and Ni on the stable and metastable transformation temperatures. In particular, it is noted that the addition of 1 wt-%Ni is expected to decrease these temperatures by $\sim$30°C. Values of T_α and T_p are reported in Table 3 and allow to express the undercooling for the stable $\Delta T_\alpha = (T_\alpha - T_{\alpha,exp})$ and for the metastable $\Delta T_p = (T_p - T_{p,exp})$ transformations. It is seen that the ΔT_α values are of the same order for TA cups varying between 29·6 and 38·3°C. For keel blocks, because of the difficulty in estimating the beginning of the transformation, the values are more scattered between 2·7 and 14·2°C. Interestingly enough, an evolution of the values of ΔT_p appears quite evident, i.e. it is strongly decreased with Ni addition. This trend is certainly related to the pearlite promoting effect sometimes reported for this element and is presently studied by differential thermal analysis.

For studying the effect of Ni on the properties of ferritic alloys, all second keel blocks have been submitted to a subcritical annealing. After preliminary trials, 6 h holding at 720°C followed by a cooling at 55 K h^{-1} to 372°C and then air cooling was adopted. Results from the metallographic observations are listed in Table 2. It is seen that the nodule count increases slightly with respect to the as cast state, with now a reasonable value for T5. The ferritising treatment has been successful in that the matrix of all materials is nearly fully ferritic with an amount of pearlite less than 2%. Figure 3*a* shows a typical microstructure of alloy T6 while Fig. 3*b* presents the aspect of the remaining pearlite that appears spheroidised. A crude estimate of the ferrite GS was evaluated on the heat treated materials by linear intercepts of five randomly selected grains. These values are reported in Table 2 where it is seen that GS varies in a very limited range, 40–65 µm, and thus should not affect the mechanical properties.

Table 3 Characteristic temperatures evaluated on cooling curves, °C

Casting	Alloy	$T_{e,min}$	T_{eut}	ΔT_{eut}	$T_{\alpha,exp}$	T_α	ΔT_α	$T_{p,exp}$	T_{trans}	T_p	ΔT_p
TA cups	T1	1136·2	1154·5	18·3	726·8	763·5	36·7	720·2	722·5	753·7	33·7
	T2	1136·7	1155·3	18·6	732·6	770·5	37·9	722·9	724·2	760·0	37·1
	T3	1139·0	1155·9	16·9	735·3	773·6	38·3	725·1	725·1	762·6	37·5
	T4	1142·1	1155·6	13·5	708·3	737·9	29·6	698·8	701·6	723·7	24·9
	T5	1139·7	1156·9	17·2	709·1	746·6	37·5	…	700·3	731·2	30·9
	T6	1141·7	1161·9	20·2	…	…	…	…	…	…	…
Keel blocks	T1	1150·2	1154·5	4·3	752·4	763·5	11·1	738·6	739·0	753·7	15·1
	T2	1150·7	1155·3	4·6	767·8	770·5	2·7	…	748·3	760·0	11·7
	T3	1149·2	1155·9	6·7	763·3	773·6	10·3	…	752·3	762·6	10·3
	T4	1150·0	1155·6	5·6	734·4	737·9	3·5	716·6	717·2	723·7	8·1
	T5	1150·8	1156·9	6·1	732·8	746·6	14·2	722·8	723·3	731·2	8·4
	T6	1153·7	1161·9	8·2	739·4	749·5	10·1	…	730·4	734·1	3·7

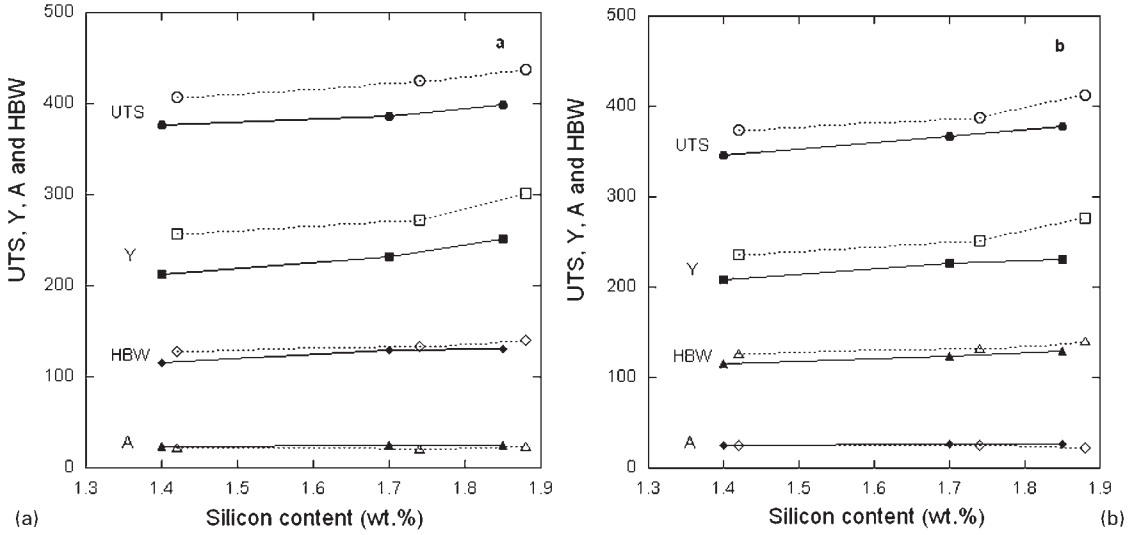

4 Room temperature mechanical properties of *a* as cast and *b* heat treated materials as function of silicon content: solid symbols are for Ni free alloys; open symbols are for Ni bearing ones

The results obtained from mechanical tests are listed in Table 4 for both as cast and heat treated materials. Room temperature tensile properties and hardness are plotted in Fig. 4*a* (as cast) and Fig. 4*b* (heat treated). As expected from the previous review,[11] the values of UTS and *Y* increase by about 50–100 MPa per percent of Si, in both the as cast and heat treated states. Their absolute values are however lower for the fully ferritic matrix than for the ferritic–pearlitic ones, certainly in relation with the presence of pearlite in the as cast materials. It is noteworthy that both as cast and heat treated materials have high elongation at rupture which does not appear to decrease with Si as observed for higher Si contents.[11] The heat treatment with the associated dissolution of pearlite increases slightly the *A* values by 1–2% though such a change is below the standard experimental error. Similarly, the heat treatment does not seem to affect the hardness of the material which slightly increases with the Si content, as expected.

Focusing now on the effect of Ni, it is seen that 1 wt-%Ni increases *Y*, UTS and HBW by about 5–10% for both as cast and heat treated materials. The values of *A* are slightly lower for Ni bearing alloys than for Ni free alloys in the as cast state while they are equal after heat treatment. To sum up, an addition of 1 wt-%Ni to low silicon nodular cast irons is beneficial, increasing by 5–10% UTS, *Y* and HBW without affecting *A*.

Figure 5 shows the evolution of the average impact energy measured on as cast and heat treated alloys. For the as cast materials it is seen that the highest impact properties at RT were found in the samples without Ni. This may be due to the higher pearlite content in the materials with Ni. As the temperature is decreased to -20°C, the data for Ni bearing and Ni free materials get closer but separate again at -40°C. At -60°C, below the ductile to brittle transition, all values are very low at 5 ± 1 J. As expected from the literature,[3] the alloy with the lowest Si content of each series shows the highest impact energy at -40°C.

After heat treatment, the values of the impact energy are increased at RT and -20°C, changed either positively or negatively at -40°C and remained nearly unchanged at -60°C as seen in Fig. 5*b*. Again, the two alloys with the lowest Si content (T1 and T4) present the best properties. To stress the effect of Ni on impact properties, Fig. 6 shows all the data obtained from these two low Si alloys with tentative transition curves drawn through the corresponding average values at each

Table 4 Results obtained from mechanical tests on as cast and heat treated keel blocks

	Impact energy/J															
Melt	$T=22^{\circ}$C			$T=-20^{\circ}$C			$T=-40^{\circ}$C			$T=-60^{\circ}$C			UTS/MPa	*Y*/MPa	*A*/%	HBW
As cast																
T1	16	16	15	15	14	13	12	14	10	5	5	5	377	212	24·1	116
T2	16	16	16	11	12	12	9	11	6	5	6	5	386	232	25·3	129
T3	17	16	16	11	10	14	8	9	9	5	4	6	398	251	25·4	130
T4	13	14	13	12	12	10	10	9	8	5	8	5	407	257	22·2	128
T5	10	14	13	13	13	12	6	7	6	5	4	4	425	272	21·3	134
T6	15	14	14	12	11	13	8	6	7	6	5	4	437	301	23·2	140
Heat treated																
T1	20	19	19	18	17	17	15	13	8	6	4	6	346	208	25·7	116
T2	18	18	18	14	18	19	7	5	11	6	6	5	367	226	26·2	124
T3	17	18	20	20	15	17	7	8	10	6	6	5	378	231	26·4	129
T4	15	17	17	15	17	17	12	13	8	9	7	5	373	236	25·0	127
T5	17	16	16	13	13	16	8	12	6	6	4	5	387	252	25·6	132
T6	16	16	17	11	10	15	7	6	4	6	5	5	413	276	22·8	140

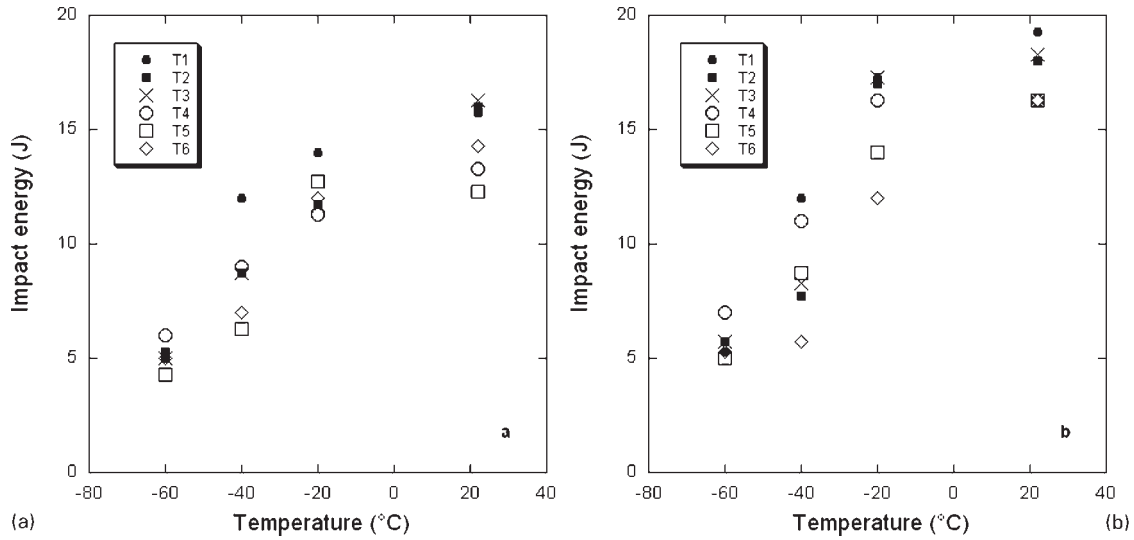

5 Effect of temperature on impact energy of *a* as cast and *b* heat treated alloys: solid symbols are for Ni free alloys; open symbols are for Ni bearing ones

temperature. It then seems that Ni additions could be beneficial at very low temperature.

Conclusions

A series of low silicon cast irons, without and with 1 wt-%Ni addition was prepared for investigating the formation of the as cast microstructure and for characterising mechanical properties of as cast and ferritised materials. The observed effect of Ni addition can be summarised as a slight increase in nodule counts and as a noteworthy increase in pearlite fraction in TA cups and keel blocks. Cooling curves recorded from Ni bearing alloys show higher eutectic arrests and lower eutectoid transformation temperatures when compared to the Ni free alloys. Both observations can be rationalised by considering the effect of Ni on the stable eutectic and stable and metastable eutectoid temperatures. Undercooling of the pearlite transformation has been observed to be very low for Ni-bearing alloys and this is presently under further investigation.

As for mechanical properties, an addition of 1 wt-%Ni to low silicon nodular cast iron is beneficial, increasing by 5–10% UTS, *Y* and HBW without affecting *A*, in either as cast and ferritised states. Furthermore, it seems that such an addition to a low Si cast iron could lead to improved impact properties at very low temperatures in the fully ferritic state.

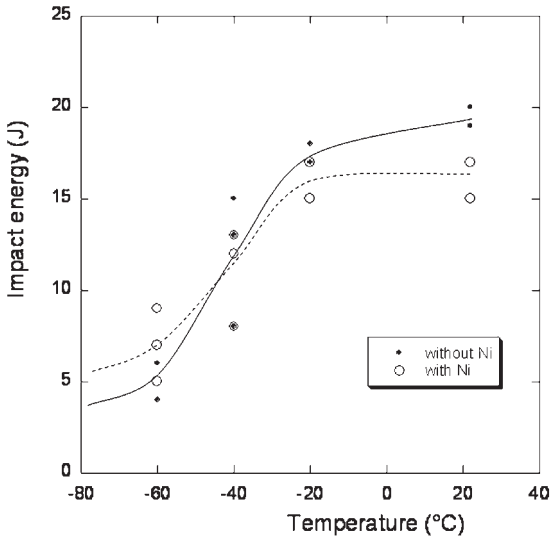

6 Effect of temperature on impact energy of heat treated low Si alloys with (T4) and without Ni (T1): all available data are shown and lines drawn go through corresponding average values at each temperature

Acknowledgement

The authors would like to thank Thermal Quality Control (TQC) Technologies and its staff for all the collaboration in the experimental work.

References

1. W. C. Leslie: *Metall. Trans.*, 1972, **3**, 5–26.
2. J. R. Davis (ed.): 'Cast irons: ASM specialty handbook', 54–79; 1996, Materials Park, OH, ASM International.
3. H. T. Angus: 'Cast iron: physical and engineering properties', 210; 1976, London, Butterworths.
4. T. Nobuki, M. Hatate and T. Shiota: *Int. J. Cast Met. Res.*, 2008, **21**, 31–38.
5. J. R. Davis (ed.): 'Cast irons: ASM specialty handbook', 65–66; 1996, Materials Park, OH, ASM International.
6. G. S. Cho, K. H. Choe, K. W. Lee and A. Ikenaga: *J. Mater. Sci. Technol.*, 2007, **23**, 97–101.
7. S. K. Yu and C. R. Loper: *AFS Trans.*, 1988, **96**, 811–822.
8. D. Venugopalan and A. Alagarsamy: *AFS Trans.*, 1990, **98**, 395–400.
9. G. H. Hsu, M. L. Chen and C. J. Hu: *Mater. Sci. Eng. A*, 2007, **A444**, 339–346.
10. J. Serrallach, J. Lacaze, J. Sertucha, R. Suárez and A. Monzón: *Key Eng. Mater.*, 2011, **457**, 361–366.
11. J. Sertucha, J. Lacaze, J. Serrallach, R. Suárez and F. Osuna: *Mater. Sci. Technol.*, 2012, **28**, 184–191.
12. J. Yamabe, M. Takagi and T. Matsui: *Tech. Rev.*, 2005, **15**, 42–51.
13. J. Asensio-Lozano and J. F. Álvarez-Antolín: *J. Mater. Eng. Perform.*, 2008, **17**, (2), 216–223.
14. J. Sertucha, P. Larrañaga, J. Lacaze and M. Insausti: *Int. J. Metalcast.*, 2010, **4**, 51–58.
15. B. Sundman, B. Jansson and J.-O. Andersson: *CALPHAD*, 1985, **9**, 153.
16. Thermo-calc software AB, www.thermocalc.com
17. J. Lacaze, C. Wilson and C. Bak: *Scand. J. Metall.*, 1994, **23**, 151–163.
18. J. Lacaze, A. Boudot, V. Gerval, D. Oquab and H. Santos: *Metall. Mater. Trans. A*, 1997, **28A**, 2015–2025.
19. J. Lacaze and V. Gerval: *ISIJ Int.*, 1998, **38**, 714–722.